Journal Homepage: -www.journalijar.com
INTERNATIONAL JOURNAL OF ADVANCED RESEARCH (IJAR)
Article DOI:10.21474/IJAR01/8479
DOI URL: http://dx.doi.org/10.21474/IJAR01/8479
ISSN NO. 2320-5407

RESEARCH ARTICLE

TRANSFORMATION OF NATURAL ANALCIME AND PHILLIPSITE DURING THEIR HYDROTHERMAL RECRYSTALLIZATION INTO ZEOLITES A AND X.

Vladimer Tsitsishvili, Nanuli Dolaberidze, Nato Mirdzveli, Manana Nijaradze, Zurab Amiridze, Nino Sinauridze, Tekla Kapanadze and Ketevan Virsaladze.
Petre Melikishvili Institute of Physical and Organic Chemistry of Ivane Javakhishvili Tbilisi State University, Tbilisi, Georgia.

Manuscript Info

Manuscript History
Received: 02 December 2018
Final Accepted: 04 January 2019
Published: February 2019

Key words:-
Hydrothermal crystallization, Zeolites A and X, Analcime, Phillipsite.

Abstract

The objective of the present work was to study transformation of Georgian natural zeolites, analcime and phillipsite, during their recrystallization in the aim to obtain zeolites A and X, widely used for adsorption, separation, ion exchange and catalysis. It is found that phase-pure zeolite NaA ($Na_{11.25(25)}$ $(K,½Ca,½Mg)_{0.7(1)}$ $(Al_{11.95(25)}Si_{12.3(3)}O_{48})\cdot 18H_2O$) can be prepared in the form of cubic/rhombus crystallites with uniform micrometric (3-5 μm) dimensions by hydrothermal crystallization (95°C) of aged (72 hr) at room temperature gel ($4.5Na_2O$: $0.45Al_2O_3$: $1SiO_2$: $178H_2O$) obtained from natural analcime, treated with hydrochloric acid before suspending in water and mixing with sodium hydroxide. Phase-pure zeolite NaX ($|Na_{66(3)}$ $[K,½Ca,½Mg,½Cu,½Zn]_{12(1)}$ $(H_2O)_{248(10)}|$ $(Al_{78(3)}Si_{114(4)}O_{384})$) with specific surface area of 589 m^2/g and total pore volume of 0.578 cm^3/g can be prepared in the form of octahedral crystallites with uniform micrometric (2-7 μm) dimensions by hydrothermal crystallization (95°C) of aged (96 hr) at room temperature gel ($2.9Na_2O$: $0.26Al_2O_3$: $1SiO_2$: $150H_2O$) obtained from water suspension of natural phillipsite, treated with hydrochloric acid and mixed with sodium hydroxide. The resulting zeolites in their characteristics are competitive with commercially available materials.

Introduction:-

Zeolites are porous crystalline aluminosilicates built from alternating SiO_4 and AlO_4^- tetrahedrons. Zeolites have been the focus of intensive activity and growth in applications over the past 30 years in adsorption, ion exchange and catalytic technologies due to their excellent properties of uniform and precise nano-scale porosity, molecular shape selectivity, ion-exchange capacity, strong Brønsted acidity and high thermal and hydrothermal stability. Of the 46 natural zeolites, clinoptilolite is the most studied and widely used, and of more than two hundred synthetic zeolites, the A, X and Y zeolites find the greatest practical application, and this is described in detail in modern review articles (Mintova et al., 2015; Ennaert et al., 2016; Li et al., 2017; Bacakova et al., 2018).

Zeolite A (the crystal chemical formula $|Na_{12}$ $(H_2O)_{27}|_8$ $[Al_{12}Si_{12}O_{48}]_8$-**LTA**) has a 3-dimensional pore structure (Fig 1) with channels running perpendicular to each other in the x, y, and z planes. Crystal structure is constructed of 4-,

Corresponding Author:-Vladimer Tsitsishvili.
Address:-Petre Melikishvili Institute of Physical and Organic Chemistry of Ivane Javakhishvili Tbilisi State University, Tbilisi, Georgia.

6-, and 8-member ring secondary building units (SBUs), composite building units (CBUs) are **d4r** (cube or double 4-membered ring containing 8 T atoms (T = Si or Al)), **sod** (truncated octahedron or sodalite cage containing 24 T atoms), and **lta** containing 48 T atoms (Baerlocher et al., 2007).

Zeolite X (Si/Al<3) and zeolite Y (Si/Al>3) are analogues of the rare natural zeolite faujasite (the crystal chemical formula $|(Ca,Mg,Na_2)_{29}\ (H_2O)_{240}|$ **[**$Al_{58}Si_{134}O_{384}$]-**FAU**) having the largest unit cell (cubic, a=24.74Å) containing 192 T-atoms. Channels in the FAU crystal structure are running perpendicular to each other in the x, y, and z planes similar to LTA (Fig 1), and are made of 4- and 6-member ring SBUs, CBUs are d6r (double 6-membered ring containing 12 T atoms) and sod (Baerlocher et al., 2007). The channel diameter is large at 7.4Å since the aperture is defined by a 12-member ring, and leads into a larger cavity of diameter 12Å. The cavity is surrounded by ten sodalite cages connected on their hexagonal faces.

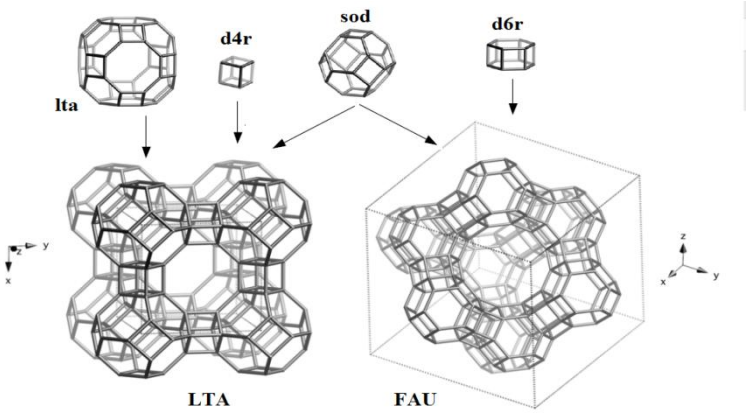

Fig 1:- Composite building units, LTA framework viewed along [001], and FAU framework viewed along [111] (Baerlocher et al., 2007).

As a commercial material, zeolite A is used in spacio-specific catalysis, especially in paraffin cracking, in ion exchange separation (Izidoro et al., 2013), and in detergents as a water-softening builder (Hul and Chao, 2006). Recently, it was found (Milenkovic et al., 2017; Dolaberidze et al., 2018) that the bactericidal activity of copper-containing zeolite A toward Escherichia coli is determined not only by the released Cu^{2+} ions, but also by the influence of the metal-containing zeolite itself.

Zeolites X and Y are used in many applications such as removal of heavy metals from aqueous waste (Izidoro et al., 2013; Ltaief et al., 2015), separation of gases in permanent gas-flow (Bastani et al., 2013), aerobic digestion process (Montalvo et al., 2012), oxidation of olefins (Bagherzadeh and Zare, 2012), mild hydrocracking of naphthenic compounds (Park et al., 2013), hydrocracking of vacuum gas oil (Cui et al., 2013) and other catalytic applications: zeolite Y is widely used in acidic form in petroleum refinery catalytic cracking units to increase the yield of gasoline and diesel fuel from crude oil feedstock by cracking heavy paraffins into gasoline grade napthas. Zeolite Y has superseded zeolite X in this use because it is both more active and more stable at high temperatures due to the higher Si/Al ratio.

Zeolites A, X and Y are conventionally synthesized with sodium silicate and aluminate through hydrothermal crystallization (Balkus and Ly, 1991) at 70-300ºC; modern practice of zeolite synthesis includes microwave (Sapawe et al, 2013) and ultrasound assisted methods (Bukhari et al., 2015), accelerated crystallization of via hydroxyl free radicals (Feng et al., 2016) and other tools (Abdullahi et al., 2017). The hydrothermal zeolite synthesis through transformation of natural silicates and industrial wastes has been used due to the search for cheap alumina and silica sources.

There have been many studies on synthesizing zeolites from natural minerals, such as smectite (Abdmeziem and Siffert, 1994), perlite (Christidis et al., 1999; Dolaberidze et al., 2018a), diatomite (Sanhueza et al., 2004; Yao et al., 2018), kaolinite (Farzaneh et al., 1989; Lin et al., 2004; San Cristóbal et al., 2010; Belviso et al., 2013; Gougazeh and Buhl, 2014; Abdullahi et al., 2017; Alaba et al., 2017; Garshasbi et al., 2017), bentonite (Garshasbi et al., 2017), feldspar (Su et al., 2016; Garshasbi et al., 2017), natural zeolites (Tsitsishvili et al., 2016a, b; Dolaberidze et al.,

2017) and other precursors (Chen et al., 2012; Purnomo et al., 2012; Wang et al., 2013; Ma et al., 2014; Li et al., 2015).

Zeolites have been also synthesized from the solid wastes, such as coal fly ash (Shigemoto et al., 1990; Morayama et al., 2002; Querol et al., 2002; Tanaka et al., 2003; Inada et al., 2005; Terzano et al., 2005; Hui and Chao, 2006; Juan et al., 2009; Babajide et al., 2012; Musyoka et al., 2015; Volli and Purkait, 2015; Yao et al., 2015; Hu et al, 2017), cupola slag (Anuwattana et al., 2008; Anuwattana and Khummongkol, 2009), oil shale ash (Shawabkeh et al., 2004; Machado and Miotto, 2005), rice husk ash (Shoumkova and Stoyanova, 2013; Manadee et al., 2017) and coal gangue (Qian and Li, 2015), but the uncertainty in their supplies and the impurity in their components may limit their practical application (Yao et al., 2018).

Natural zeolites have a fairly constant composition and controlled impurities, so that they can be used to produce synthetic zeolites. Recently it was shown (Tsitsishvili et al., 2016a), that zeolites with high silicon content and low ion exchange capacity, such as mordenite (|$Na_8(H_2O)_{24}$| **[**$Al_8Si_{40}O_{96}$**]-MOR**) type materials can be obtained by hydrothermal recrystallization of the Georgian natural clinoptilolite (empirical formula of used samples – $(Na_{3.3}K_{1.15}Ca_{0.75}Mg_{0.25}[Me]_{0.55})(Al_{7.0}Si_{29.3}O_{72})\cdot 22.5H_2O$, crystal chemical formula |$Ca_4(H_2O)_{24}$| **[**$Al_8Si_{28}O_{72}$**]-HEU**) in the absence of seeds and organic templates, but materials with high aluminium content and ion exchange capacity, like the LTA and FAU type zeolites can be obtained only by two-stage recrystallization of raw: natural zeolite firstly was transformed in the sodalite (|Na_8Cl_2| **[**$Al_6Si_6O_{24}$**]-SOD**) structure, and then in the target product (Tsitsishvili et al., 2016b; Dolaberidze et al., 2017). The reason for such behavior may be a comparatively high Si/Al ratio (>4.0) in raw material, so to produce the A and X zeolites, it is better to use common zeolites with a comparatively low Si/Al ratio, such as chabazite (Si/Al=3.0), analcime and laumontite (Si/Al=2.0), or phillipsite (Si/Al=$^5/_3$). Another reason for the impossibility of recrystallization of clinoptilolite in zeolite A may be the fact that the HEU structure has only 4-member ring SBU of 4– 4=1 type containing 9 T-atoms, and CBU of bre type containing 10 T-atoms.

The aim of our work was to study the recrystallization of the Georgian natural zeolites analcime and phillipsite to obtain the A and X zeolite structures in one step without application of crystallization seeds and organic templates. Analcime structure contains 4- and 6-member ring SBUs, has no CBUs and may be suitable for the preparation of zeolite A. Phillipsite has 4- and 8-member ring SBUs, double crankshaft chain as CBU and may be applied to obtain zeolite X. Both zeolites are widespread in Georgia, but have no practical application.

Materials and Methods:-

Materials:-

Preparation of synthetic zeolite materials was carried out using following Georgian natural zeolites described and characterized (Tsitsishvili et al., 1998) previously:

1. analcime from Chachubeti, Eastern Georgia, with chemical composition characterized by empirical formula $(Na_{10.8}K_{1.52}Ca_{0.64}Mg_{0.40}[Me]_{0.9})(Al_{15.3}Si_{33.0}O_{96})\cdot 16H_2O$ (Me = Fe, Cu, etc.) and zeolite phase content of approx. 70%, major impurities – chlorite and montmorrilonite;
2. phillipsite from the Akhaltsikhe field, Southern Georgia, with chemical composition expressed by formula $(Na_{1.36(3)}K_{0.70(2)}Ca_{0.70(3)}Mg_{0.32(1)}[Me]_{0.10(1)})(Al_{4.2}Si_{11.5}O_{32})\cdot 12H_2O$ (Me = Fe, Cu, Zn, etc.), zeolite phase content up to 70%, major impurities – quartz and clay minerals.

Sodium hydroxide and the other chemicals used in the experiments were purchased from Merck KGaA (Darmstadt, Germany). All chemicals were of analytical reagent grade and used without any further purification. Deionized water was used throughout this study.

Preparation of zeolites:-

Processing of raw in target material included following steps: preparation of material, preparation of suspension, gel formation and aging, hydrothermal crystallization, and separation of product.

In the experiments were used zeolite-containing rocks, crushed in the planetary micro mill Pulverisette 7 premium line (Fritsch Laboratory Instruments, Idar-Oberstein, Germany) to a size less than 0.063 mm (250 BSS mesh).

Analcime powder was treated at room temperature by HCl water solution (12%) under stirring, washed by water before the complete disappearance of Cl^- ions, and dried in thermostat oven at 100-105^oC; water suspension (the

solid to liquid ratio of 1 : 3) of homogeneous amorphous (XRD tested) material was prepared in Teflon flack; suspension was treated at room temperature by NaOH water solution (20%) under stirring, homogenization and gel formation takes approx. 30 minutes.

Phillipsite powder was suspended in Teflon flack placed in shaking water bath OLS 26 Aqua Pro (Grant Instruments, Cambridge, UK) controlling temperature at 90-95^{o}C; suspension was processed with a 12% hydrochloric acid solution at the rate of 5 mL per gram of the solid raw material; activated suspension was diluted with water and treated by adding of a 25% sodium hydroxide solution, followed by the formation of a homogeneous gel for about one hour.

General characteristics of the target zeolite products are in strong dependence on the chemical composition of gel ($aNa_2O{\cdot}bAl_2O_3{\cdot}SiO_2{\cdot}cH_2O$) prepared for aging and crystallization: the Si/Al ratio determines the type of porous structure to be produced; application of sodium hydroxide provides an alkaline environment for breaking T–O bonds and gives possibility to prepare nearly pure sodium forms; high water content ensures suitable viscosity and other physical properties for crystallization process. The molar ratios SiO_2/Al_2O_3, Na_2O/Al_2O_3, and H_2O/ Na_2O, optimal for obtaining zeolite A from analcime and zeolite X from phillipsite, are given in the Table 1.

The aging of the gel in all cases was carried out at room temperature for several days; crystallization was carried out in temperature-controlled water bath; the temperature (up to 95^{o}C) and duration have been adjusted to prepare micrometric single crystals with diameter of 2-8 μm. The crystallization was followed by X-ray diffraction (XRD) patterns, the strongest peaks (2Θ~30° for zeolite A, according to recent results (Dolaberidze et al., 2017), and 2Θ = 6.1° for zeolite X) were observed to detect the start of zeolitization and determine the time of formation of a stable structure, shown in the Table 1.

Separation of produced crystalline material was carried out by filtration of mother solution, solid material was cleaned by distilled water until pH 8.0-8.5, and dried at 90-100^{o}C.

Table 1:- Optimal chemical composition of the gel, duration of its aging and crystallization

Raw material	Chachubeti analcime	Akhaltsikhe phillipsite
Target product structure	LTA	FAU
Molar ratio SiO_2/Al_2O_3	2.2	3.8
Molar ratio Na_2O/Al_2O_3	9.8	12
Molar ratio H_2O/Na_2O	40	55
Gel aging duration, hr	72	96
Beginning of zeolitization, hr after start	30	16
Total crystallization time, hr	up to 120	up to 55

Characterization:-

Chemical composition of raw material and prepared samples was determined by elemental analyses carried out using a 381L plasma spectrometer (Spectromom, Hungary) and atomic absorption spectrometer (model 300, Perkin-Elmer, UK), as well as by energy dispersive X-ray (EDS) analysis. The crystalline phase was identified by powder X-ray diffraction (XRD) patterns obtained from a modernized Dron-4 X-ray diffractometer (Russia) employing the Cu-K_α line (λ = 0.154056 nm). The samples were scanned in the 2Θ range of 5^{o} to 50^{o} with a 0.02^{o} step at a scanning speed of 1^{o}/min. Fourier transform infrared (FT-IR) spectra were collected by a Perkin-Elmer 10.4.2 FTIR spectrometer (UK) over the range of 400–4000 cm^{-1} with a resolution of 2 cm^{-1} using the KBr pellet technique for sample preparation. The surface morphology of the samples was observed by scanning electron microscope JSM6510LV (Jeol, Japan) equipped with X-Max 20 analyzer (Oxford Instruments, UK) for EDS. Nitrogen adsorption-desorption isotherms were measured at 77 K using an ASAP 2020 Plus physisorption analyzer (Micromeritics, Norcross, GA, USA), after evacuation of the samples at 350^{o}C.

Results and Discussion:-

XRD characterization and chemical composition:-

Numerous studies listed in the reviews (Bukhari et al., 2015; Abdullahi et al., 2017) have found that, regardless of the raw materials and crystallization technique, the reactant ratios of SiO_2/Al_2O_3 and Na_2O/SiO_2 in the reaction mixture (gel) are crucial parameters to determine the crystallinity and properties of the zeolite products from

hydrothermal synthesis. Using analcime pre-activated with hydrochloric acid and forming a gel in accordance with the amounts of sodium and water given in Table 1, zeolite A can be obtained with a high degree of phase purity. This is confirmed by the powder XRD pattern (Fig 2), which corresponds to the XRD pattern of zeolite A, obtained from the rice husk ash and aluminium scrap (Shoumkova and Stoyanova, 2013), and characterized by high intensity peaks at 2Θ = 7, 10, 12, 16, 21, 24, 27, 30, and 34°. No additional diffraction peaks have been observed at 2Θ = 14.5 and 25° indicating the possible formation of a thermodynamically more stable structure of sodalite, as in the case of high-temperature synthesis of zeolite A from coal fly ash (Hu et al., 2017). Experimental XRD pattern of target product has been compared with calculated one taken from the "Database of Zeolite Structures" of the International Zeolite Association Structure Commission (http://www.iza-structure.org/). Calculated XRD pattern include a large number of low-intensity peaks that are not observed experimentally, so for comparison with recorded pattern only peaks of comparatively high intensity (over 0.09Imax) have been taken into consideration. As a result, the following assignment of diffraction peaks at corresponding 2Θ° (relative intensity I/Imax in %; hkl; d spacing in Å) was made: 2Θ = 7.2° (51%;200;12.3Å), 10.1° (38%;220;8.7Å), 12.4° (24%;222;7.1Å), 16.2°(22%;420;5.5Å), 21.1°(8%;600;4.2Å), 21.8°(46%;442;4.1Å), 24.0°(80%;622;3.7Å), 26.0°(20%;620;3.4Å), 26.9°(82%;642;3.3Å), 29.9°(100%;820+644;2.98Å), 32.9°(42%;840;2.75Å), and 34.2°(74%;664;2.62Å). It is impossible to unambiguously assign a peak at 2Θ = 30.08°, as well as peaks for which the 2Θ angle exceeds 35 degrees. With the exception of peak intensities, these data are in full agreement with previously published results for zeolite A, obtained by two-step recrystallization of clinoptilolite (Dolaberidze et al., 2017).

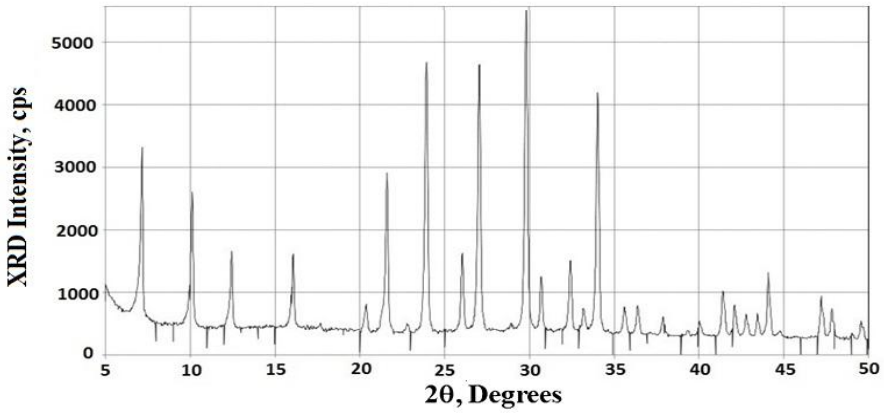

Fig 2:- Experimental XRD pattern of the material obtained from the recrystallization of analcime.

The chemical composition of zeolite A, obtained from natural analcime, is described by the empirical formula $Na_{11.25(25)}(K,½Ca,½Mg)_{0.7(1)}(Al_{11.95(25)}Si_{12.3(3)}O_{48})\cdot 18H_2O$, and is in a good accordance with corresponding crystal chemical formula $|Na_{12}(H_2O)_{27}|_8[Al_{12}Si_{12}O_{48}]_8$ with the exception of small "lack" of the Al atoms (Si/Al=1.03±0.025) in the frame as in a case of two-stage crystallization (Tsitsishvili et al., 2016b). Samples of zeolite A obtained from kaolin usually have Si/Al values from 1.15 (Alkan et al., 2005; Ríos Reyes et al., 2010) to 1.3 (Ugal et al., 2010), although it was reported about application (Georgiev et al., 2014) and preparation (Kazemimoghadam and Mohammadi, 2006; Melo et al., 2012) of zeolite 4A with Si/Al ~1.

The XRD pattern of phillipsite recrystallization product (Fig 3) shows not only the strongest peak at 2Θ = 6.1° (100%;111;14.28Å), but also all low intensity peaks given in the "Database of Zeolite Structures" for hydrated NaX zeolite: 2Θ = 10° (9%;220;8.75Å), 11.8° (7.5%;311;7.46Å), 15.4° (11%;331;5.7Å), 18.5° (4%;551;4.8Å), 20° (4%;440;4.38Å), 22.4° (1%;620;4.5Å), 23.3° (6.5%;533;3.8Å), 26.6° (7%;642;3.3Å), 29.2° (2.5%;733;3.05Å), 30.3° (3%;822;2.95Å), 31° (6%;555;2.85Å), 32° (3%;840;2.75Å), 33.6° (3%;664;2.65Å), 37.4° (2%;666;2.35Å), 40.8° (1.5%;880;2.17Å), and 41.3° (1.5%;955;2.15Å). Peaks at larger 2Θ angles cannot be attributed unambiguously, but their positions and intensities coincide with those published for a commercial zeolite and a sample synthesized from pure chemicals (Masoudian et al, 2013).

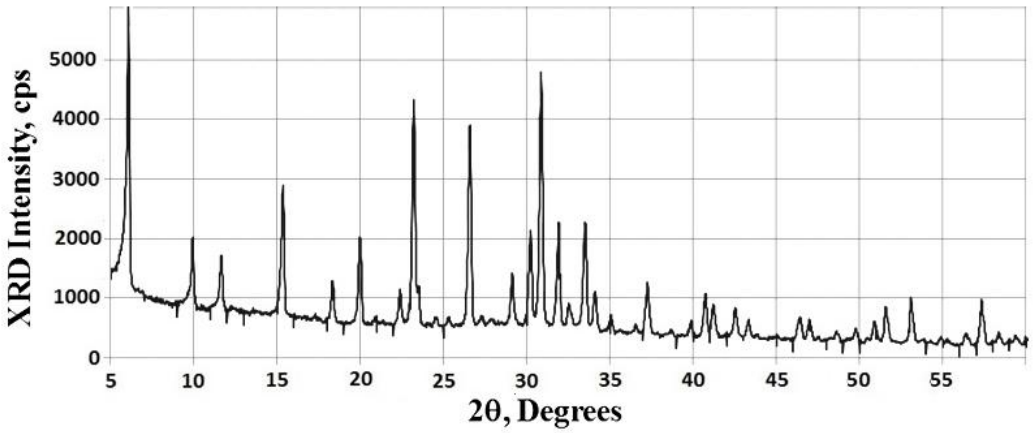

Fig 3:- Experimental XRD pattern of the material obtained from the recrystallization of phillipsite.

It can be seen that the main crystalline phase is zeolite X, no peaks of zeolite A have been observed.
According to the data of the elemental and EDS analysis, counted on 384 oxygen atoms and 192 T-atoms in the unit cell, the empirical formula of the obtained compound can be represented as $|Na_{66(3)}\ [Me]_{12(1)}\ (H_2O)_{248(10)}|\ (Al_{78(3)}Si_{114(4)}O_{384})$ (Me = K, ½Ca, ½Mg, ½Cu and ½Zn, the latter is unevenly distributed). Compared to the crystal chemical formula of FAU with $(Al_{58}Si_{134}O_{384})$ and $(H_2O)_{240}$, the resulting compound has elevated aluminum content and reduced silicon content with about the same number of crystallization water molecules. Module Si/Al = 1.46±0.07, and the resulting material can be attributed to zeolite NaX.

Optimal conditions and parameters of transformation:-
Obtaining of zeolite NaX from a gel with molar ratio SiO_2/Al_2O_3 = 3.8 corresponds to the results of a previous study (Zhang et al., 2013), according to which a single phase NaX zeolite was obtained from sodium silicate and sodium aluminate only with the SiO_2/Al_2O_3 molar ratio of 1.5–4.0. When using pure chemicals, the NaA zeolite was developed at SiO_2/Al_2O_3 = 1.0 in addition to the NaX zeolite, but at SiO_2/Al_2O_3 = 0.5 a single phase NaA zeolite was generated. However, the use of natural precursors leads to other results, the synthesis of zeolite X from coal fly ash was carried out at SiO_2/Al_2O_3 = 5, and zeolite A at SiO_2/Al_2O_3 = 1.67 (Hu et al., 2017), so that the preparation of zeolite NaA by recrystallization of analcime at SiO_2/Al_2O_3 = 2.2 and large molar ratio Na_2O/Al_2O_3 is understandable.

Generally, high alkaline concentration of the crystallization system accelerates the dissolution of silicon and aluminum components in the precursor materials (Cundy et al., 2005). The optimal conditions for the recrystallization of the analcime in zeolite A were the ratios $4.5Na_2O/SiO_2$ and $\sim 40H_2O/Na_2O$, while the synthesis of the same zeolite from the coal fly ash was successfully carried out at significantly lower sodium content ($1.3Na_2O/SiO_2$) partially compensated by comparatively low dilution factor, $1.3Na_2O/SiO_2$ (Hu et al., 2017). In all likelihood, such a high alkaline concentration is needed to transform the structure of analcime, which has the highest framework density (18.5T/1000Å^3) among zeolites (Baerlocher et al., 2007).

The optimal conditions for the recrystallization of the phillipsite in zeolite X are $2.9Na_2O/SiO_2$ and $\sim 50H_2O/Na_2O$. The same zeolite was synthesized from the coal fly ash at lower sodium content $2.2Na_2O/SiO_2$ compensated by comparatively low dilution, $\sim 40H_2O/Na_2O$ (Hu et al., 2017), synthesis of zeolite X from diatomite was carried out in conditions of slightly higher sodium content ($3.0Na_2O/SiO_2$) and lower dilution factor, $40H_2O/Na_2O$ (Yao et al., 2018). Structure PHI has a rather low framework density (15.8T/1000Å^3), and high alkalinity is not needed for its transformation.

Aging also plays an important role in the nucleation of amorphous gel. During this stage, the aluminosilicate species included in the gel phase are transformed along with the aging conditions (Ogura et al., 2003). In the study, out of considerations of energy saving, the room temperature was chosen for aging the gel. Of course, this led to a significant increase in the duration of aging, from about six to ten hours to several days, but this saves more than 100 Joules per gram of the reaction mixture. The same energy saving considerations were taken into account when selecting the optimum crystallization temperature. In addition, it was decided to carry out recrystallization at a temperature below the boiling point of water, in this case there is no need to use an autoclave.

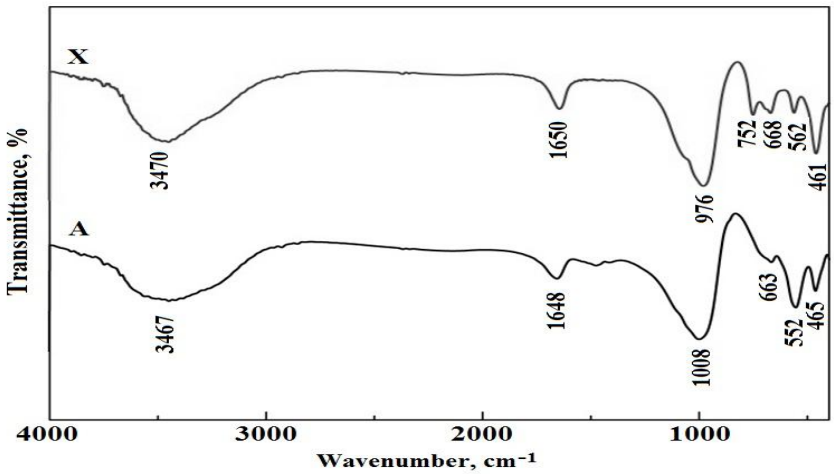

Fig 4:- FT-IR spectra of obtained zeolites NaA (A) and NaX (X).

FT-IR characterization:-

The mid infra red peak patterns in FTIR spectra (Fig 4) testify formation of zeolite structure in both cases. The band of the internal deformation vibration modes of T-O-T bridges and the band of the internal vibration of T-O symmetric stretching have little influence from the Si/Al ratio: transmittance peaks were recorded at 465 and 663 cm^{-1} for zeolite NaA, and at 461 and 668 cm^{-1} for zeolite NaX, respectively. The band associated with the asymmetric external vibration of double four-rings of zeolite framework is more sensitive to the Si/Al ratio: 552 cm^{-1} for zeolite NaA, and 562 cm^{-1} for zeolite NaX. The band of valence T–O–T vibrations gives peak at 752 cm^{-1} only for zeolite NaX. The internal vibration of T-O asymmetric stretching gives peak at 1008 cm^{-1} for the NaA sample, for zeolite NaX it is shifted to the lower wave numbers (976 cm^{-1}) due to increased silicon content (Mozgawa et al., 1999).

In both spectra, bands are observed at ~1650 and ~3470 cm^{-1} corresponding to the presence of H_2O and hydroxyls, respectively. The observed FT-IR bands are in good agreement with those reported previously for zeolite A (Sapawe et al, 2013; Jiang et al., 2016), zeolite X (Flanigen et al, 1971; Wang et al., 2013) and both (Hu et al., 2017), which further proves the successful synthesis of zeolites NaA from analcime and NaX from phillipsite.

Sorption properties:-

Developed zeolite crystal microporous structure in synthesized samples has been confirmed also by their sorption properties. The N_2 adsorption-desorption plot at 77 K for the prepared zeolite NaX is presented in Fig 5 and corresponds to typical Langmuir isotherm with the presence of steep nitrogen uptake at very low relative pressures (p/p_o~0.05), which is attributed to the filling of micropores.

The calculated specific surface area, 589 m^2/g, is comparable to 573 m^2/g for zeolite X, obtained from coal fly ash (Hu et al., 2017), and is greater than the specific surface area of 453 m^2/g reported for NaX obtained from diatomite (Yao et al., 2018).

The total pore volume of prepared NaX is 0.578 cm^3/g, the volume of micropores with a diameter of less than 8 Å is 0.301 cm^3/g, which is slightly higher than the volume of micropores in zeolites X obtained from coal fly ash (0.281 cm^3/g) and from diatomite (0.284 cm^3/g). It is noted (Chen et al., 2016) that such a volume of micropores is much higher than that of NaX zeolites synthesized with structure-directing reagents which block some of the channels.

Type H_1 (Sing et al., 1985) narrow hysteresis loop, corresponding to the filling of well defined cylindrical pore channels, is observed at high relative pressures (from 0.9 to 0.99); average channel diameter calculated by the Brunauer-Emmett-Teller (BET) method is 67 nm, by the Barrett-Joyner-Halenda (BJH) method – 58 (adsorption) and 53 (desorption) nm.

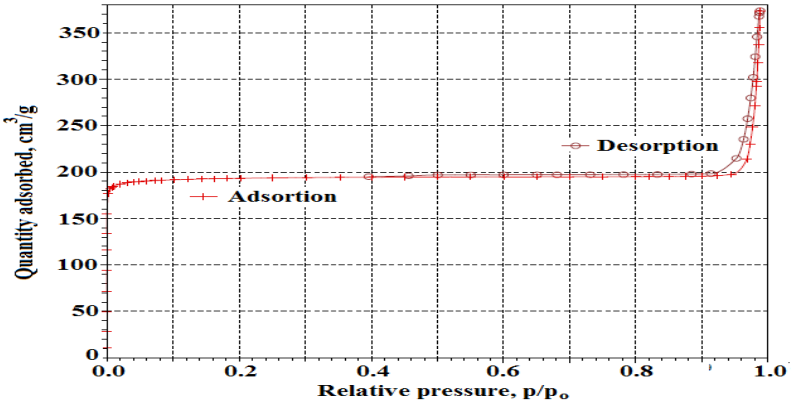

Fig 5:- N_2 adsorption-desorption isotherms of NaX.

The loop observed in the synthesized zeolite NaX is different from the wide hysteresis loops described for some synthetic zeolites (Ltaief et al., 2015; Yao et al., 2018) and corresponding to the filling of disordered pores (type H_2) or uniform slit-shaped (type H_3) intercrystal mesopores of non-rigid aggregates of plate-like particles, ascribed to the packing of zeolite crystals.

The maximum adsorption capacity of synthesized NaX measured for water vapor is up to 0.394 cm^3/g, which is more than indicated for a commercial sample (0.3303 cm^3/g), but water adsorption capacity of micropores (measured under static conditions at the "plateau" pressure p/p_0=0.40) is only 0.2052 cm^3/g, up to 48% of water molecules are adsorbed in mesopores.

In structure LTA, the pore size (0.41 nm) is much smaller than that of the FAU structure and is similar to the kinetic diameter of N_2 (0.364 nm), so the BET surface area of the synthesized NaA sample was not measured; water adsorption capacity of micropores (p/p_0=0.40) is up to 0.24 cm^3/g and is consistent with most of the reports on phase-pure zeolite NaA.

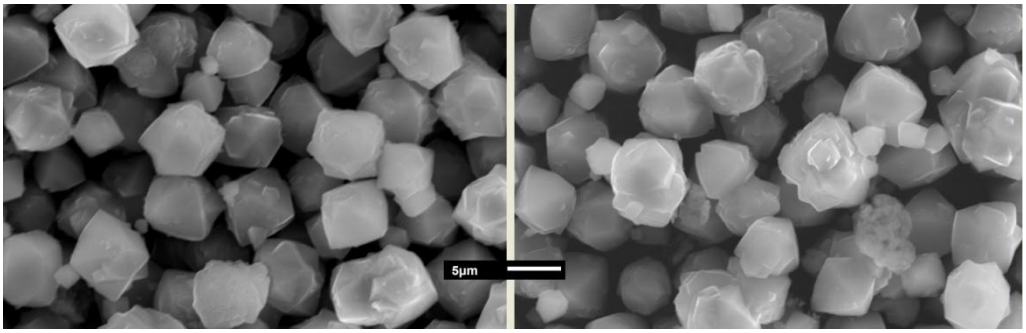

Fig 6:- SEM images (x2,700) of zeolite NaA (left) and zeolite NaX (right).

SEM images:-

The SEM images of NaA and NaX are shown in Fig 6. In general, more than 92% of NaA crystallites have uniform size of 3 – 5 µm and cubic or rhombus morphology, as well as more than 95% of NaX crystallites have octahedral habit and uniform size of 2 – 7 µm.

In the process of synthesizing zeolite NaA, a small amount (<3wt.%) of spherical or ellipsoidal nanoscale (average diameter 0.25 µm) crystallites is also formed, while long crystallization of NaX results in micrometric crystals combined into honeycomb-like structure through nanocrystal bridges. However, obtaining of "hierarchical" zeolites is the task of our subsequent research.

Conclusion:-

It is of great significance to develop cheap, energy-saving and eco-friendly routines that can synthesize zeolites A and X from low-cost raw materials.

In this study, zeolite NaA with chemical composition $Na_{11.25(25)}(K,½Ca,½Mg)_{0.7(1)}(Al_{11.95(25)}Si_{12.3(3)}O_{48})\cdot 18H_2O$ and high phase purity was synthesized from pre-treated with hydrochloric acid natural analcime by suspending it in water and forming a gel with sodium hydroxide; the gel had $4.5Na_2O$: $0.45Al_2O_3$: $1SiO_2$: $178H_2O$ composition, its aging at room temperature lasted 72 hours, product formation begins after 40 hours, complete hydrothermal crystallization at 95^oC lasts up to 120 hours.

Zeolite NaX with chemical composition $|Na_{66(3)}\ [K,½Ca,½Mg,½Cu,½Zn]_{12(1)}\ (H_2O)_{248(10)}|\ (Al_{78(3)}Si_{114(4)}O_{384})$ was obtained from natural phillipsite suspended in water and treated with hydrochloric acid; the gel ($2.9Na_2O$: $0.26Al_2O_3$: $1SiO_2$: $150H_2O$) was aged at room temperature for 96 hours, the formation of the product began after 16 hours, complete hydrothermal crystallization at 95^oC lasted up to 55 hours.

The structure, as well as high phase purity and crystallinity of both samples is confirmed by their X-ray diffraction patterns and FT-IR spectra. Zeolite NaX is characterized by high specific surface area (589 m^2/g) and pore volume (0.578 cm^3/g) including micropores of LTA structure (52%) and cylindrical channels with diameter up to 67 nm (48%). SEM observation revealed that most of the NaA and NaX crystallites have uniform micrometric size.

Acknowledgements:-

This work was supported by Shota Rustaveli National Science Foundation of Georgia (SRNSFG) [grant number FR17_187]. The authors thank Vakhtang Gabunia for help with X-ray studies and Giorgi Tsintskaladze for helping with the characterization of zeolites by IR spectroscopy.

References:-

1. Abdmeziem, K. and Siffert, B. (1994). Synthesis of large crystals of ZSM-5 zeolite from smectite clay mineral. Applied Clay Science, 8: 437-447.
2. Abdullahi, T., Harun, Z. and Othman, M.H.D. (2017). A review on sustainable synthesis of zeolite from kaolinite resources via hydrothermal process. Advanced Powder Technology, 28: 1827-1840.
3. Alaba, P.A., Sani, Y.M., Mohammed, I.Y., Abakr, Y.A. and Daud, W.M.A.W. (2017). Synthesis and characterization of sulfated hierarchical nanoporous faujasite zeolite for efficient transesterification of shea butter. J. Clean. Prod., 142: 1987-1993.
4. Alkan, M., Hopa, Ç., Yilmaz, Z. and Güler, H. (2005). The effect of alkali concentration and solid/liquid ratio on the hydrothermal synthesis of zeolite NaA from natural kaolinite. Microporous Mesoporous Mater., 86: 176-184.
5. Anuwattana Jr., R., Balkus, K.J., Asavapisit, S. and Khummongkol, P. (2008). Conventional and microwave hydrothermal synthesis of zeolite ZSM-5 from the cupola slag. Microporous and Mesoporous Materials, 111: 260-266.
6. Anuwattana, R. and Khummongkol, P. (2009). Conventional hydrothermal synthesis of Na-A zeolite from cupola slag and aluminum sludge. Journal of Hazardous Materials, 166: 227-232.
7. Babajide, O., Musyoka, N., Petrik, L. and Ameer, F. (2012). Novel zeolite Na-X synthesized from fly ash as a heterogeneous catalyst in biodiesel production. Catal. Today, 190: 54-60.
8. Bacakova, L., Vandrovcova, M., Kopova, I. and Jirka I. (2018). Applications of zeolites in biotechnology and medicine – a review. Biomaterials Sci., 6: 974-989.
9. Baerlocher, Ch., McCucker, L.B. and Olson, D.H. (2007) Atlas of Zeolite Framework Types. Sixth revised Edition. Elsevier, Amsterdam, pp. 142-143.
10. Bagherzadeh, M. and Zare, M. (2012). Synthesis and characterization of NaY zeolite-encapsulated Mn-hydrazone Schiff base: an efficient and reusable catalyst for oxidation of olefins. Journal of Coordination Chemistry, 65(22): 4054-4066.
11. Balkus, K.J. and Ly, K.T. (1991). The preparation and characterization of an X-type zeolite. An experiment in solid state chemistry. Journal of Chemical Education, 68(10): 875-877.
12. Bastani, D., Esmaeili, N., Asadollahi, M. (2013). Polymeric mixed matrix membranes containing zeolites as a filler for gas separation applications: A review. Journal of Industrial and Engineering Chemistry. 19: 375-393.

13. Belviso, C., Cavalcante, F., Lettino, A. and Fiore, S. (2013). A and X-type zeolites synthesised from kaolinite at low temperature. Appl. Clay Sci., 80-81: 162-168.
14. Bukhari, S.S., Behin, J., Kazemian, H. And Rohani, S. (2015). Conversion of coal fly ash to zeolite utilizing microwave and ultrasound energies: a review. Fuel, 140: 250-266.
15. Chen, D., Hu, X., Shi, L., Cui, Q., Wang, H. and Yao, H. (2012). Synthesis and characterization of zeolite X from lithium slag. Appl. Clay Sci., 59-60: 148-151.
16. Chen, Y., Xu, T., Xie, C., Han, H., Zhao, F., Zhang, J., Song, H. and Wang, B. (2016). Pure zeolite Na-P and Na-X prepared from coal fly ash under the effect of steric hindrance. J. Chem. Technol. Biotechnol., 91: 2018-2025.
17. Christidis, G.E., Paspaliaris, I. and Kontopoulos, A. (1999). Zeolitisation of perlite fines: mineralogical characteristics of the end products and mobilization of chemical elements. Applied Clay Science, 15: 305-324.
18. Cui, Q., Zhou, Y., Wei, Q., Yu, G. and Zhu, L. (2013). Performance of Zr- and P-modified USY-based catalyst in hydrocracking of vacuum gas oil. Fuel Processing Technology, 106: 439-446.
19. Cundy, C.S. and Cox, P.A. (2005). The hydrothermal synthesis of zeolites: Precursors, intermediates and reaction mechanism, Micropor. Mesopor.Mat., 82: 1-78.
20. Dolaberidze, N.M., Tsitsishvili, V.G., Mirdzveli, N.A. and Nijaradze, M.O. (2017). Synthesis of LTA type zeolites from Georgian clinoptilolite. Chemistry, Physics and Technology of Surface (Ukraine), 8: 346-350.
21. Ennaert, T., Van Aelst, J., Dijkmans, J., De Clercq, R., Schutyser, W., Dusselier, M., Verboekend, D. and Sels, B.F. (2016). Potential and challenges of zeolite chemistry in the catalytic conversion of biomass. Chem. Soc. Rev., 45: 584–611.
22. Farzaneh, F., Oskooie, M.K. and Nejad, M.M.A. (1989). The synthesis of zeolites A, X and HS from natural Iranian kaolinite and the study of the transformation of zeolites X to HS and zeolites Y to P by X-ray diffraction and scanning electron microscopy. Journal of Sciences – Islamic Republic of Iran, 1: 23-28.
23. Feng, G., Cheng, P., Yan, W., Boronat, M., Li, X., Su, J.-H., Wang, J., Li, Y., Corma, A., Xu, R. and Yu, J. (2016). Accelerated crystallization of zeolites via hydroxyl free radicals. Science, 351: 1188–1191.
24. Flanigen, E.M., Khatami, H. and Szymanski, H.A. (1971). Infrared structural studies of zeolite frameworks. Adv. Chem. Ser., 101: 201-229.
25. Garshasbi, V., Jahangiri, M. and Anbia, M. (2017). Equilibrium CO_2 adsorption on zeolite 13X prepared from natural clays. Appl. Surf. Sci., 393: 225-233.
26. Georgiev, D., Petrov, I., Mihalev, T., Peychev, I., Gradinarov, I. and Kolchakova, G, (2014). Granulation of natural zeolite. Scientific, 53: 51-55.
27. Gougazeh, M. and Buhl, J.-Ch. (2014). Synthesis and characterization of zeolite A by hydrothermal transformation of natural Jordanian kaolin. Journal of the Association of Arab Universities for Basic and Applied Sciences, 15: 35-42.
28. Hui, K.S. and Chao, C.Y.H. (2006). Pure, single phase, high crystalline, chamfered-edge zeolite 4A synthesized from coal fly ash for use as a builder in detergents. Journal of Hazardous Materials, 137(1): 401-409.
29. Hu, T., Gao, W., Liu, X., Zhang. Y. and Meng, C. (2017). Synthesis of zeolites Na-A and Na-X from tablet compressed and calcinated coal fly ash. Royal Society Open Science, 4(10): 170921-170934.
30. Inada, M., Eguchi, Y., Enomoto, N. and Hojo, J. (2005). Synthesis of zeolites from coal fly ashes with different silica-alumina composition. Fuel, 84: 299-304.
31. Izidoro, J.D.C., Fungaro, D.A., Abbott, J.E. and Wang, S. (2013). Synthesis of zeolites X and A from fly ashes for cadmium and zinc removal from aqueous solutions in single and binary ion systems. Fuel, 103: 827-834.
32. Jiang, Z., Yang, J., Ma, H., Ma, X. and Yuan, J. (2016). Synthesis of pure NaA zeolites from coal fly ashes for ammonium removal from aqueous solutions. Clean Technol. Environ. Policy, 18: 629-637.
33. Juan, R., Hernandez, S., Andres, J.M. and Ruiz, C. (2009). Ion exchange uptake of ammonium in wastewater from a sewage treatment plant by zeolitic materials from fly ash. Journal of Hazardous Materials, 161: 781-786.
34. Kazemimoghadam, M. and Mohammadi, T. (2006). Preparation of NaA zeolite membranes for separation of water/UDMH mixtures. Separation and Purification Technologies, 47: 173-178.
35. Li, C., Zhong, H., Wang, S., Xue, J. and Zhang, Z. (2015). Removal of basic dye (methylene blue) from aqueous solution using zeolite synthesized from electrolytic manganese residue. J. Ind. Eng. Chem., 23: 344-352.
36. Lin, D., Xu, X., Zuo, F. and Long, Y. (2004). Crystallization of JBW, CAN, SOD and ABW type zeolite from transformation of meta-kaolin. Microporous and Mesoporous Materials, 70: 63-70.
37. Li, Y., Li, L. and Yu, J. (2017) Applications of Zeolites in Sustainable Chemistry. Chem, 3: 928-949.

38. Ltaief, O.O., Siffert, S., Fourmentin, S. and Benzina, M. (2015). Synthesis of faujasite type zeolite from low grade Tunisian clay for the removal of heavy metals from aqueous waste by batch process: Kinetic and equilibrium study. Comptes Rendus Chimie, 18: 1123-1133.
39. Machado, N.R.C.F. and Miotto, D.M.M. (2005). Synthesis of Na-A and X zeolites from oil shale ash. Fuel, 84: 2289-2294.
40. Ma, D., Wang, Z., Guo, M., Zhang, M. and Liu, J. (2014). Feasible conversion of solid waste bauxite tailings into highly crystalline 4A zeolite with valuable application. Waste Manag., 34: 2365-2372.
41. Manadee, S., Sophiphun, O., Osakoo, N., Supamathanon, N., Kidkhunthod, P., Chanlek, N., Wittayakun, J. and Prayoonpokarach, S. (2017). Identification of potassium phase in catalysts supported on zeolite NaX and performance in transesterification of Jatropha seed oil. Fuel Process. Technol., 156: 62-67.
42. Masoudian, S.K., Sadighi, S. and Abbasi, A. (2013). Synthesis and characterization of high aluminum zeolite X from technical grade materials. Bulletin of Chemical Reaction Engineering & Catalysis, 8(1): 54-60.
43. Melo, C.R., Riella, H.G., Kuhnen, N.C., Angioletto, E., Melo, A.R., Bernardin, A.M., da Rocha, M.R. and da Silva, L. (2012). Synthesis of 4A zeolites from kaolin for obtaining 5A zeolites through ionic exchange for adsorption of arsenic. Mater. Sci. Eng., B177: 345-349.
44. Milenkovic, J., Hrenovicm J., Matijasevic, D., Niksic, M., and Rajic, N. (2017). Bactericidal activity of Cu-, Zn-, and Ag-containing zeolites toward Escherichia coli isolates. Environmental Science and Pollution Research, 24: 20273–20281.
45. Mintova, S., Jaber, M., and Valtchev, V. (2015). Nanosized microporous crystals: emerging applications. Chem. Soc. Rev., 44: 7207–7233.
46. Montalvo, S., Guerrero, L., Borja, R., Sánchez, E., Milán, Z., Cortés, I. and Rubias, M. A. (2012). Application of natural zeolites in anaerobic digestion processes: A review. Applied Clay Science, 58: 125-133.
47. Morayama, N., Yamamoto, H. and Shibata, J. (2002). Mechanism of zeolite synthesis from coal fly ash by alkali hydrothermal reaction. International Journal of Mineral Processing, 64: 1-17.
48. Mozgawa, W., Sitarz, M. and Rokita, M. (1999). Spectroscopic studies of different aluminosilicate structures. Journal of Molecular Structure, 511-512: 251-257.
49. Musyoka, N.M., Ren, J., Langmi, H.W., North, B.C. and Mathe, M. (2015). A comparison of hydrogen storage capacity of commercial and fly ash-derived zeolite X together with their respective templated carbon derivatives. Int. J. Hydrog. Energy, 40: 12705-12712.
50. Ogura, M., Kawazu, Y., Takahashi, H. and Okubo, T. (2003). Aluminosilicate species in the hydrogel phase formed during the aging process for the crystallization of FAU zeolite. Chem. Mater., 15: 2661-2667.
51. Park, J., Ahmed Ali, S., Alhooshani, K., Azizi, N., Miyawaki, J., Kim, T., Lee, Y., Kim, H.S., Yoon, S.H. and Mochida, I. (2013). Mild hydrocracking of 1-methyl naphthalene (1-MN) over alumina modified zeolite. Journal of Industrial and Engineering Chemistry, 19: 627-632.
52. Purnomo, C.W., Salim, C. and Hinode, H. (2012). Synthesis of pure Na–X and Na–A zeolite from bagasse fly ash. Microporous Mesoporous Mater., 162: 6-13.
53. Qian, T. and Li, J. (2015). Synthesis of Na-A zeolite from coal gangue with the in-situ crystallization technique. Adv. Powder Technol., 26: 98-104.
54. Querol, X., Moreno, N., Umana, J.C., Alastuey, A., Hernandez, E. and Lopez-Soler, A. (2002). Synthesis of zeolite from coal fly ash: an overview. International Journal of Coal Geology, 50: 413-423.
55. Ríos Reyes, C.A., Williams, C.D. and Castellanos Alarcón, O.M. (2010). Synthesis of zeolite LTA from thermally treated kaolinite. Revista Facultad de Ingenieria Universidad de Antioquia, 2010: 30-41.
56. San Cristóbal, A.G., Castelló, R., Martín Luengo,M.A. and Vizcayno, C. (2010). Zeolites prepared from calcined and mechanically modified kaolins: A comparative study. Applied Clay Science, 49: 239-246.
57. Sanhueza, V., Kelm, U., Cid, R. and López-Escobar, L. (2004). Synthesis of ZSM-5 from diatomite: a case of zeolite synthesis from a natural material. Journal of Chemical Technology and Biotechnology, 79: 686-690.
58. Sapawe, N., Jalil, A.A., Triwahyono, S., Shah, M.I.A., Jusoh, R., Salleh, N.F.M., Hameed, B.H. and Karim, A.H. (2013). Cost-effective microwave rapid synthesis of zeolite NaA for removal of methylene blue. Chemical Engineering Journal, 229: 388-398.
59. Shawabkeh, R., Al-Harahsheh, A., Hami, M. and Khlaifat, A. (2004). Conversion of oil shale ash into zeolite for cadmium and lead removal from wastewater. Fuel, 83: 981-985.
60. Shigemoto, N., Hayashi, H. and Miyaura, K. (1990). Selective formation of Na-X zeolite from coal fly ash by fusion with sodium hydroxide prior to hydrothermal reaction. Journal of Materials Research, 28: 4781-4786.
61. Shoumkova, A. and Stoyanova, V. (2013). SEM–EDX and XRD characterization of zeolite NaA, synthesized from rice husk and aluminium scrap by different procedures for preparation of the initial hydrogel. Journal of Porous Materials, 20(1): 249-255.

62. Sing, K.S.W., Everett, D.H., Haul, R.A.W., Moscou, L., Pierotti, R.A., Rouquérol, J. and Siemieniewska, T. (1985). Reporting physisorption data for gas/solid systems with special reference to the determination of surface area and porosity. Pure Appl. Chem., 57: 603-612.
63. Su, S., Ma, H. and Chuan, X. (2016). Hydrothermal synthesis of zeolite A from K-feldspar and its crystallization mechanism. Adv. Powder Technol., 27: 139-144.
64. Tanaka, H., Matsumura, S., Furusawa, S. and Hino, R. (2003). Conversion of coal fly ash to Na-X zeolites. Journal of Materials Science Letters, 22: 323-325.
65. Terzano, R., Spagnuoloa, M., Medici, L., Tateo, F. and Ruggiero, P. (2005). Zeolite synthesis from pre-treated coal fly ash in presence of soil as a tool for soil remediation. Applied Clay Science, 29: 99-110.
66. Tsitsishvili, V., Dolaberidze, N., Mirdzveli, N. and Nijaradze, M. (2016a). MOR type synthetic zeolite material. Proceedings of Georgian National Academy of Sciences, chemical series, 42(1): 35-39.
67. Tsitsishvili, V., Dolaberidze, N., Alelishvili, M., Nijaradze, M. and Mirdzveli, N. (2016b). New generation zeolitic adsorbers. Proceedings of Georgian National Academy of Sciences, chemical series, 42(3): 276-280.
68. Tsitsishvili, V., Dolaberidze, N., Alelishvili, M., Tsintskaladze, G., Sturua, G., Chipashvili, D., Nijaradze, M. and Khazaradze, N. (1998). Adsorption and thermal properties of zeolitic rocks from newly investigated deposit plots in Georgia. Georgian Eng. News, 2(6): 61-65.
69. Ugal, J.R., Hassan, K.H. and Ali, I.H. (2010). Preparation of type 4A zeolite from Iraqi kaolin: characterization and properties measurements, J. Assoc. Arab Univ. Basic Appl. Sci., 9: 2-5.
70. Volli, V. and Purkait, M.K. (2015). Selective preparation of zeolite X and A from flyash and its use as catalyst for biodiesel production. J. Hazard. Mater., 297: 101-111.
71. Wang, C., Zhou, J., Wang, Y., Yang, M., Li, Y. And Meng, C. (2013). Synthesis of zeolite X from low-grade bauxite. J. Chem. Technol. Biotechnol, 88: 1350-1357.
72. Yao, G., Lei, J., Zhang, X., Sun, Z. and Zheng, S. (2018). One-step hydrothermal synthesis of zeolite X powder from natural low-grade diatomite. Materials, 11: 906-920.
73. Yao, Z.T., Ji, X.S., Sarker, P.K., Tang, J.H., Ge, L.Q., Xia, M.S. and Xi, Y.Q. (2015). A comprehensive review on the applications of coal fly ash. Earth Sci. Rev., 141: 105-121.
74. Zhang, X., Tang, D., Zhang, M. and Yang R. (2013). Synthesis of NaX zeolite: Influence of crystallization time, temperature and batch molar ratio SiO_2/Al_2O_3 on the particulate properties of zeolite crystals. Powder Technology, 235: 322-328.